

# Effect of Airflow on Rate of Paper Yellowing in Dark Storage Test Conditions

Matthew Comstock, Ann McCarthy, Paul Sacoto, and Rebecca Silveston-Keith; Lexmark International, Inc.; Lexington, Kentucky, USA

## Abstract

*It is well known that inkjet photographic prints can be susceptible to fading due to environmental factors such as light, ozone, humidity, and temperature; moreover, that these environmental factors interact differently depending on the ink and paper chemistry. Image permanence test methods typically involve separate image permanence evaluations for each environmental factor by imposing strict requirements on the non-active factors present in each test setup. This approach is necessary because the impacts of combining several such environmental effects together in a storage environment are difficult to control and model in a repeatable way. As a part of defining the required test conditions, it is necessary to correctly identify and constrain each environmental factor that can impact test results. In particular, this study probes the interacting effects of temperature and airflow on inkjet microporous photo paper samples, and the ways in which these interactions can impact image permanence evaluation of prints for dark (photo album) storage conditions. This research has been conducted as a contribution to the developing ISO standardized test method for image permanence applicable to consumer dark storage conditions.*

## Introduction

The life expectancy for printed photos stored in albums or other protected 'dark' enclosures can be estimated using tests that evaluate the print permanence response to accelerated ozone, humidity, and thermal (dark storage) conditions. Print permanence response to accelerated thermal conditions can be evaluated using the Arrhenius method as described in various dark stability tests [1, 2]. The method requires testing samples at a range of elevated temperatures, the results of which are then used to extrapolate life predictions at an assumed typical consumer storage temperature. Dark stability tests require a large commitment of resources to test. A single test at each temperature takes weeks, months, and sometimes years to reach failure. The process can be sped up by using several test chambers simultaneously, each at a different temperature. As a result, significant effort is necessary to understand and control each influencing factor in the test setup and methodology.

The primary failure modes with traditional silver halide print materials are colorant optical density (OD) failure and substrate yellowing. In the case of digital printing, failure modes may differ. Lexmark's latest generation pigmented inks are robust against colorant migration on a variety of media, so the typical failure mode for prints using these inks in dark stability tests is an increase in blue density due to paper yellowing. The precise failure mode is the color imbalance between the red and blue densities in the  $D_{min}$  patch (i.e. unprinted substrate surface), which in the proposed ISO

image life standard draft, is listed as an allowable change in OD of 0.10 [3].

Because of the resources involved in dark stability testing, and because the failure mode has historically been distributed across ink and media changes, not much scrutiny has been placed on the method's results for this type of  $D_{min}$  only failure.

Recently the inkjet digital printing industry has shifted the technology used in photo media from a swellable to a microporous ink receiving layer. Coincidentally, testing has shown that it is difficult to get consistent results in this type of  $D_{min}$  only failure in dark stability tests. The shift in paper technology explains part of the observed instability in the paper yellowing test results. This research report will show that the rate of microporous paper yellowing is influenced by the airflow while tests of swellable media have not demonstrated this interaction with airflow.

## Experiment

The following equipment was used in the dark stability testing:

- Gretag Spectrolino/Spectroscan for density measurements
- ESPEC ESL-4CW for environmental control
- Kahn Optidew Bench chilled mirror hygrometer
- Testo 445 hot bulb anemometer
- Specially built blower tubes to control airflow

Three separate environmental chambers were used in testing and all were the same model with an interior capacity of one cubic meter. These chambers used solid state humidity sensors. All were calibrated with respect to a NIST traceable chilled mirror hygrometer and calibration was repeated each time the chamber set point was changed. The blower tubes (see Figure 1) had a diameter of 8 inches and were composed of three distinct sections held together with mesh tubing to allow different airflows along the length of the tube.

Test samples were 6x12 cm unprinted commercially available microporous media (hereafter referred to as Media A, B, C, and D) which had been pre-screened from a larger list of candidates to identify thermal susceptibility. Normally 2 measurements per sample are taken. In this experiment, 36 measurements were taken on each sample at 1 cm increments (a 4x9 grid of size 3x8 cm) and averaged. The additional measurements are used to evaluate measurement variability.

Samples were mounted in different configurations. There were free hanging samples (FH) in accordance with ISO 18909, samples wrapped with standoff brackets within aluminum foil (AL), and samples mounted with tape inside special blower tubes (BT2, BT4, BT6) with the backsides of the samples directly in contact with the aluminum tube.

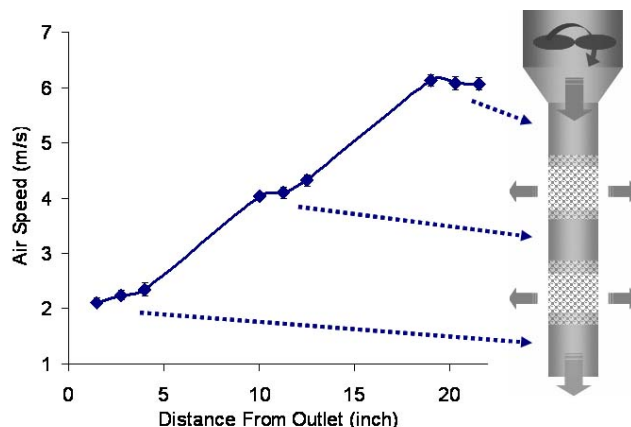


Figure 1. Blower unit illustration and air velocity measurements.

The samples were handled with gloves to avoid any potential contamination. Moreover, most samples were measured the same day as they were removed from the chamber.

Samples were tested at 3 different temperatures: 92C, 85C, and 78C; and a standard 50%RH. These high temperatures were chosen to accelerate the thermal reaction, as the fastest yellowing photo media identified would take half a year to fail at lower temperatures. Even at these high temperatures, there was not enough time to reach failure for all samples. The frequency of measurements was a function of the test temperature and the length of time the test had already run. Three or four measurements were taken on each sample.

The measured airflow in the chamber used for the FH samples was  $1\pm0.5\text{m/s}$ . There was no forced airflow in the case of the AL samples. Figure 1 shows the blower tube design and airflow measurements. The airflow was measured in the tubes before they were placed in the chamber. In the lower section, it was  $2\pm1\text{m/s}$  (BT2 samples), in the middle section it was  $4\pm1\text{m/s}$  (BT4 samples) and in the upper section it was  $6\pm1\text{m/s}$  (BT6 samples). These measurements are referred to as nominal from here on.

## Results and Discussion

For simplicity, only the yellow OD change ( $\Delta\text{OD}_y$ ) will be analyzed in this report rather than the color imbalance between the red and blue densities. Failure is defined as a 0.1 OD change, thus resulting in a slightly more conservative analysis than [2, 3].

### Measurement Variability

The  $\Delta\text{OD}_y$  for the samples was mapped in two dimensions with surface diagrams. In this manner, the progression of media degradation was monitored at each time measurement. This technique permitted analysis of experimental errors and outliers. For example, Figure 2 shows the surface mapping of a typical sample with the propagation of a single point defect at  $x = 40\text{mm}$  and  $y = 80\text{mm}$  at different time intervals.

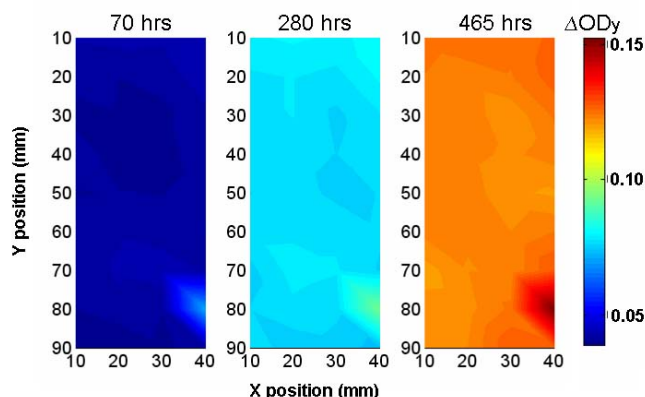


Figure 2. Media with point defect. Media C at 85C/50%RH from BT6

The large number of measurements within each sample ensured that single point defects did not introduce significant errors. Note that the effects of single point failures may not be negligible if fewer OD measurements are taken.

Because some samples were placed against metal surfaces, the variability induced by the sample backing was also evaluated. All four media were tested at 92C/50%RH with and without backing in free hanging conditions. Table 1 shows a comparison of the percent difference between backed samples and samples without backing. The difference is larger in the shorter time measurements due to the  $\Delta\text{OD}_y$  proximity to zero, and becomes practically negligible for later test points. From this data we could conclude that the backing had little impact on the test.

Table 1. Percent Difference between Samples with and without Backing

| Time(hrs) | Media Type |       |        |        |
|-----------|------------|-------|--------|--------|
|           | A          | B     | C      | D      |
| 50        | 2.83%      | 5.88% | 5.42%  | 5.12%  |
| 140       | 0.89%      | 1.98% | -0.29% | -1.85% |
| 240       | -0.40%     | 0.67% | 0.41%  | -2.37% |

Sample to sample variability was also considered by including two replicates for two of the four media tested. Table 2 shows the percent difference in  $\Delta\text{OD}_y$  for the two media at 92C/50%RH. Although few replicates were used, the data does suggest that variability between replicates is small. The FH samples are an exception and often show large percent differences between replicates, potentially due in part to variable airflow within the chamber.

Table 2. Percent Difference between Sample Replicates. At 92C/50%RH and Test End Time (240hrs)

| Airflow | Media Type |      |
|---------|------------|------|
|         | A          | B    |
| AL      | 4.0%       | 1.3% |
| FH      | 16.2%      | 6.0% |
| BT2     | 1.3%       | 1.1% |
| BT4     | 1.1%       | 0.7% |
| BT6     | 0.6%       | 4.3% |

The 92C/50%RH test was repeated in order to assess test method repeatability. Table 3 shows the percent difference in deltaODy for the two replicates. There is significant discrepancy in this case and further work is underway to better understand its source. One probable source is that after the end of the second test some samples were left exposed to office light for a few days before being measured. According to [4], exposure to light after a sample has been in a dark stability test can result in 'bleaching'. This coincides with our data for the second test which showed lower than expected deltaODy end point values for these measurements. As a consequence, the 92C/50%RH data from the repeated test is not included in the following analysis.

**Table 3. Percent Difference between Test Replicates. At 92C/50%RH and Test End Time (240hrs)**

| Airflow | Media Type |     |     |     |
|---------|------------|-----|-----|-----|
|         | A          | B   | C   | D   |
| FH      | -7%        | 6%  | -7% | -7% |
| BT2     | 10%        | 15% | 13% | 12% |
| BT4     | 0%         | 8%  | 5%  | 4%  |
| BT6     | 10%        | 27% | 11% | 12% |

### Analysis of DeltaODy vs. Time Data of Airflow Impact on Media Degradation

Generally, deltaODy showed increased yellowing with increased airflow. Figure 3 shows this trend along with one notable exception. The deltaODy of the FH samples did not correlate with the deltaODy of the BT2 samples whose airflow conditions most closely correspond to the airflow measured in the chamber. Furthermore, the FH sample deltaODy did not fit with the overall trend found in the BT samples. Free hanging samples frequently showed faster degradation than predicted by the trend in the data from the other test conditions. The reason for this phenomenon is not yet understood. Airflow variability alone can not explain the FH sample results.

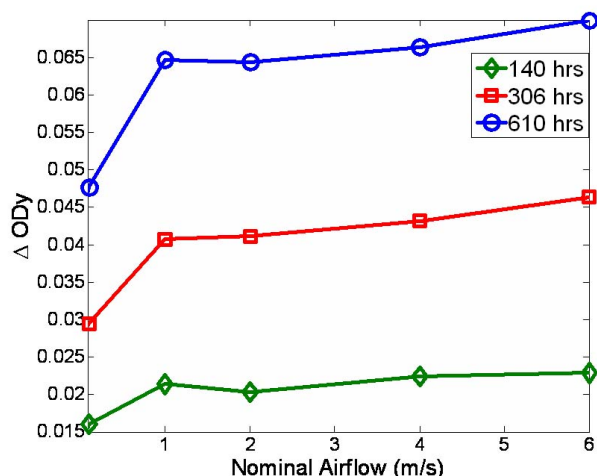


Figure 3. DeltaODy vs. nominal airflow for various measurement times. Media B at 78C/50%RH.

Linear and power law models were employed to best fit the data. Analysis of the deltaODy vs. time profile at different airflows

reveals that, generally, higher airflows result in higher non-linearity. For example, Figure 4 shows that a linear model is not the best fit for Media D. This suggests that the rate of degradation process is influenced by airflow. The power law model provides a reasonable fit to the non-linearities observed.

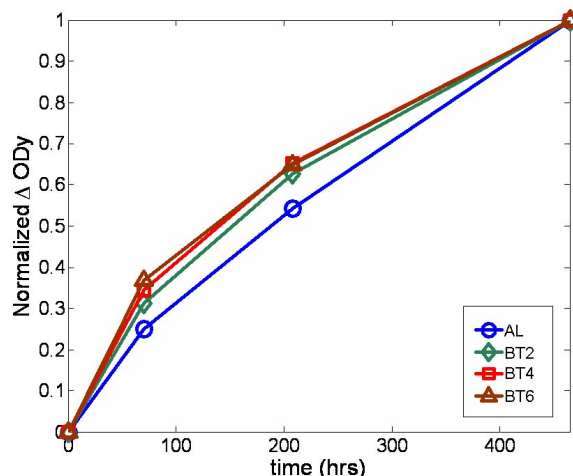


Figure 4. Normalized deltaODy vs. time profile, Media D at 85C/50%RH

Table 4 shows a comparison of predicted hours to failure, at each test temperature, using the power law as means for extrapolation/interpolation. The results consistently show that higher airflows yield faster degradation across different media and temperatures.

**Table 4. Prediction of Failure Times (Hours) by Power Law Interpolation/Extrapolation**

| T(C) | Media | Airflow |      |      |      |     |
|------|-------|---------|------|------|------|-----|
|      |       | AL      | FH   | BT2  | BT4  | BT6 |
| 78   | A     | 1137    | 693  | 665  | 623  | 607 |
| 85   | A     | 481     | 309  | 334  | 293  | 295 |
| 92   | A     | 243     | 146  | 131  | 116  | 107 |
| 78   | B     | 1627    | 1059 | 1025 | 1021 | 925 |
| 85   | B     | 785     | 515  | 572  | 538  | 517 |
| 92   | B     | 345     | 309  | 297  | 275  | 258 |
| 78   | C     | 1010    | 1091 | 911  | 896  | 869 |
| 85   | C     | 517     | 350  | 332  | 318  | 324 |
| 92   | C     | 202     | 191  | 158  | 142  | 138 |
| 78   | D     | 1042    | 974  | 889  | 815  | 795 |
| 85   | D     | 473     | 352  | 341  | 342  | 358 |
| 92   | D     | 200     | 183  | 151  | 140  | 135 |

The mechanisms behind the media degradation as a function of airflow are currently under investigation. One hypothesis is that the true culprit for the media yellowing stems from a chemical interaction between the media and atmospheric moieties such as oxygen, moisture, ozone, etc. Thus, consistent with chemical kinetics, the concentration and/or partial pressures of the environmental components coupled with the number of reacting sites in the porous structure of the media can be considered as the primary variables responsible for the dark storage failures observed in this experiment. One or more rate constants would be

required to accurately describe these mechanisms. Understanding and modeling these non-linearities involves complex heterogeneous porous reaction mechanisms which, for the moment, are outside the scope of this work.

### Analysis of Airflow Impact on Arrhenius Predictions of Media Life

Arrhenius extrapolation was used to evaluate the impact of airflow on predicted media life under dark storage conditions for microporous media. The fundamental Arrhenius relation is:

$$k = Ae^{-\frac{E}{RT}} \quad (1)$$

where  $k$  is a concentration (deltaODy) independent rate constant,  $A$  is the pre-exponential factor,  $E$  is the activation energy,  $R$  is the universal gas constant and  $T$  is the absolute temperature. The logarithm of  $k$  is linearly modeled against the inverse of temperature, and a prediction of 'failure time' is determined by extrapolation to ambient conditions (23C/50%RH for this test) [1, 2].

In our analysis, we used the linear fit model on the deltaODy vs. time data to obtain the rate constant,  $k$ , despite the fact that our earlier analysis showed that the power law fit the data better. The linear fit approach is parsimonious and provides a more conservative media life estimate. Our final analysis of media life as a function of airflow used this approach.

We also considered a simplified Arrhenius relation in which the time to failure  $t_f$  is a surrogate for  $k$ . This simplification is exact as long as the deltaODy vs. time relationship is linear with a zero intercept, and provides flexibility in estimating  $t_f$ . The equation describing this simplified method is:

$$t_f = b_0 e^{-b_1 \frac{1}{T}} \quad (2)$$

where  $b_0$  and  $b_1$  are the respective regression coefficients.

Table 5 shows predicted media life at 23C/50%RH for each sample tested as a function of nominal airflow using the fundamental Arrhenius relation. According to this evaluation, airflow has a significant impact on the media life prediction for particular media. Media A and B are greatly affected by airflow, and yet do not vary significantly at different airflow levels. This threshold behavior suggests that even a small amount of airflow contributes to the mechanisms that induce change in the media.

**Table 5. Predicted Media Life (Years) at 23C/50%RH Using the Fundamental Arrhenius Relation Method ( $R^2 > 0.975$ )**

| Media Type | Airflow |     |     |     |     |
|------------|---------|-----|-----|-----|-----|
|            | AL      | BT2 | BT4 | BT6 | FH  |
| A          | 90      | 45  | 44  | 49  | 34  |
| B          | 157     | 39  | 41  | 35  | 29  |
| C          | 237     | 190 | 217 | 176 | 134 |
| D          | 181     | 167 | 160 | 145 | 116 |

On the other hand, Media C and D display much lower initial impact due to airflow, but do show a slight trend toward decreasing media life as airflow increases.

In addition, the FH samples of Media C and D also show faster than expected degradation. More experimental data is necessary to fully explain this observation.

Tables 6 and 7 show media life predictions using the simplified Arrhenius relation with two techniques for obtaining estimates for  $t_f$ : linear interpolation/extrapolation, and power interpolation/extrapolation. The power law model provides more accurate  $t_f$  predictions at the test temperatures noted earlier.

**Table 6. Predicted Media Life (Years) at 23C/50%RH Using the Simplified Arrhenius Relation with  $t_f$  Obtained via Linear Interpolation/Extrapolation ( $R^2 > 0.993$ )**

| Media Type | Airflow |     |     |     |     |
|------------|---------|-----|-----|-----|-----|
|            | AL      | BT2 | BT4 | BT6 | FH  |
| A          | 83      | 81  | 84  | 95  | 61  |
| B          | 167     | 60  | 61  | 51  | 47  |
| C          | 289     | 275 | 320 | 257 | 189 |
| D          | 201     | 240 | 236 | 234 | 178 |

**Table 7. Predicted Media Life (Years) at 23C/50%RH Using the Simplified Arrhenius Relation with  $t_f$  Obtained via Power Law Interpolation/Extrapolation ( $R^2 > 0.990$ )**

| Media Type | Airflow |     |     |     |     |
|------------|---------|-----|-----|-----|-----|
|            | AL      | BT2 | BT4 | BT6 | FH  |
| A          | 223     | 205 | 251 | 320 | 151 |
| B          | 347     | 48  | 68  | 53  | 46  |
| C          | 292     | 489 | 741 | 728 | 537 |
| D          | 355     | 534 | 481 | 506 | 347 |

Media life predictions based on the simplified Arrhenius relation using linearly regressed  $t_f$  values are close to those produced by the fundamental Arrhenius relation. However, in some cases, the trend shown in the experimental data is not maintained when using the simplified Arrhenius relation (with linear fit) to extrapolate to long term media life prediction. Furthermore, the prediction from the simplified Arrhenius relation is counterintuitive in some cases, in which higher airflows appear to cause less yellowing.

Media life predictions based on the simplified Arrhenius relation using power law regressed  $t_f$  values deviate even further from the predictions of the preceding methods. Predicted media life times are significantly larger and difficult to rationalize.

The discrepancies observed between various Arrhenius relations are likely an effect of the inflation of experimental errors propagated through the logarithmic Arrhenius extrapolation. In addition, with the current digital media technology, the predicted media life times are several orders of magnitude larger than the test times. Because of this disparity, the extrapolation inflates the propagated errors even more and as a result trends with respect to airflow in the actual test data can reverse in the extrapolated prediction. Utilizing the fundamental Arrhenius relation coupled with the linearity assumption helped average out experimental error and did not show the model-induced features captured by the simplified Arrhenius relation. Consequently, the results from the

fundamental Arrhenius relation, with the linear fit data, are more physically meaningful, providing the best match to our observations and understanding. Furthermore, the fundamental Arrhenius relation with the linear fit data, based on the characteristics of the model, can be expected to underestimate the predicted media life. Conversely, it appears that the simplified Arrhenius relation does not behave consistently in response to non-linear experimental data.

## Conclusion

We found an impact due to airflow on the dark storage stability of glossy microporous paper. First, different sources of variability were investigated. We found that the test repeatability to be the largest source of variability. In addition, free hanging samples did not follow expected trends, showed large sample to sample variability, and inconsistency with results measured from samples under more controlled airflow conditions. The source of these observations is not fully understood and requires additional investigation. Note that the AL samples followed the expected trends, based on the BT results, for zero airflow conditions.

The deltaODy vs. time relationship was found to be non-linear and a power law model provided the best fit estimates for failure times at the elevated test temperatures. The results from the power law fit data clearly demonstrated a direct relationship between airflow and yellowing rate.

Extrapolations using the fundamental Arrhenius expression and a linear parsimonious deltaODy vs. time relationship also clearly showed a direct relationship between airflow and paper yellowing. Using this model we found that certain microporous papers have a strong initial sensitivity to even small amounts of airflow. Other papers show a gradually increasing response with increasing airflow.

In comparison, media life predictions produced by the simplified Arrhenius method differed considerably depending on the means employed to estimate failure times. Arrhenius media life predictions with the power law best fit failure times produced divergent results. The discrepancy in the results from the two Arrhenius relations was likely dominated by error propagation induced by the nature and extent of the logarithmic Arrhenius extrapolations. Further work is needed to develop improved

models that describe the relationship between dark storage stability and environmental factors such as airflow, and incorporate these findings into the fundamental Arrhenius relation.

## References

- [1] H. Scott Fogler, *Elements of Chemical Reaction Engineering*, Prentice Hall PTR; 2nd edition (1992)
- [2] ISO 18909 Photography — Processed photographic colour films and paper prints — Methods for measuring image stability
- [3] CD 1 ISO 18936 Imaging Materials – Thermal Stability of Processed Consumer Colour Photographs – Method for Testing Imaging Materials – Thermal
- [4] Henry Wilhelm, “Light-Induced and Thermally-Induced Yellowish Stain Formation in Inkjet Prints and Traditional Chromogenic Color Photographs”, Japan Hardcopy 2003, pp. 213-216.

## Author Biographies

*Matthew Comstock is responsible for the Image Permanence Lab in the Inkjet Paper, Performance, and Permanence group, Lexmark International, Inc. He received his B.S and M.S. degrees from Purdue in Mechanical Engineering in 1997 and 1999 respectively. His work is primarily focused on image permanence test method development and image permanence testing.*

*Ann McCarthy received her BS (1982) in Computer Engineering and MS (1997) in Imaging Science from the Rochester Institute of Technology. Ms. McCarthy represents Lexmark International in various international standards committees dealing with color and printing. She is Chair of I3A/IT9, the US technical committee for ISO TC42 WG5, and Chair of the International Color Consortium (ICC) Workflow WG. She is a member of the IEEE and the Society for Imaging Science and Technology (IS&T).*

*Paul Sacoto received his MS and BS in Chemical Engineering (1999) at the University of South Florida, Tampa, Florida. Paul joined Lexmark International, Inc. in 1999. His primary focus is on the study of complex ink—media interactions in the Inkjet Paper, Performance, and Permanence group.*

*Rebecca Silveston-Keith is the manager of the Inkjet Paper, Performance, and Permanence group, Lexmark International, Inc. She joined Lexmark in 2004, following more than 10 years working in physical/surface chemistry research and materials design for digital printing. Dr. Silveston-Keith received her undergraduate degree in Engineering Chemistry from Queens University in Canada (1986) and her doctorate in Chemical Engineering from Uppsala University of Sweden (1993).*